

MOLECULAR GAS IN MRK 109: CONSTRAINING THE O₂/CO RATIO IN CHEMICALLY YOUNG GALAXIES

D. T. Frayer

Astronomy Department, California Institute of Technology, Pasadena, CA 91125

E. R. Seaquist

Astronomy Department, University of Toronto, Toronto, ON, M5S 3H8, Canada

T. X. Thuan

Astronomy Department, University of Virginia, Charlottesville, VA 22903

and

A. Sievers

Institut de Radioastronomie Milliétrique, Granada, Spain

ABSTRACT

We report on observations of ¹²CO(1→0) emission from the chemically young starburst galaxy Mrk 109. These observations were part of a study to constrain the O₂/CO ratio in metal-deficient galaxies, which were motivated by theoretical work that suggests the possible enhancement of the O₂/CO ratio in chemically young systems. Five low metallicity ($Z \leq 0.5Z_{\odot}$) IRAS galaxies at redshifts $z > 0.02$ (required to shift the 118.75 GHz ¹⁶O₂ line away from the atmospheric line) were searched for CO emission. We detected the CO line in only Mrk 109. From O₂ observations of Mrk 109, we achieved an upper limit for the O₂ column density abundance ratio of $N(\text{O}_2)/N(\text{CO}) < 0.31$. These results provide useful constraints for the theoretical models of chemically young galaxies. We argue that either most of the molecular gas in Mrk 109 does not reside in dark clouds ($A_V \gtrsim 5$), or the standard equilibrium chemistry models are inadequate for metal-poor systems. The molecular gas mass implied by the CO observations of Mrk 109 is $M(\text{H}_2) \simeq 4 \times 10^9 M_{\odot}$, and the CO data are consistent with a central starburst induced by the interaction with a nearby companion.

Subject headings: galaxies: individual (Mrk109) — galaxies: ISM — galaxies: starburst

1. INTRODUCTION

Although studying the molecular gas content of metal-deficient galaxies is challenging, such efforts are essential for our understanding of the formation and evolution of galaxies. By

studying chemically young galaxies in the local universe, we gain insight into the processes which occurred at early times ($z \sim 1 - 5$) for the metal-rich spiral and elliptical galaxies found at the current epoch. Unfortunately, chemically young galaxies tend to be dwarf galaxies and are difficult to detect in CO (Combes 1985; Arnault et al. 1988; Sage et al. 1992; Israel, Tacconi, & Baas 1995). Due to the observational difficulties, very little is currently understood about the molecular gas content of chemically young galaxies. One of the main uncertainties is the CO to H₂ conversion factor. Wilson (1995) and Arimoto, Sofue, & Tsujimoto (1996) have found an empirical relationship indicating an increase in the CO to H₂ conversion factor with decreasing metallicity. However, detailed studies of the molecular clouds in the LMC and SMC suggest other factors, besides metallicity, have an important role on the CO to H₂ conversion factor (Rubio 1997; Israel 1997).

Although significant questions remain in our understanding of the CO to H₂ factor, the molecular chemistry that occurs in metal-deficient galaxies is even more uncertain. Molecular chemistry calculations are quite complicated and typically involve networks of hundreds to several thousand reactions (Graedel, Langer, & Frerking 1982; Herbst & Leung 1989 [HL89]; Langer & Graedel 1989 [LG89]; Bergin, Langer, & Goldsmith 1995 [BLG95]). Since the chemistry models still have difficulties in explaining several of the observed abundance ratios in Galactic molecular clouds, very little modeling has been devoted to metal-poor galaxies. One notable exception is the theoretical study of the chemistry in LMC and SMC molecular clouds by Millar & Herbst (1990) [MH90]. In general, the molecular chemistry models are sensitive to a variety of parameters, such as the density, temperature, and ionization field, but the dominant parameter for determining the relative molecular abundances of the carbon and oxygen species is the carbon to oxygen ratio (LG89). The models predict that the O₂/CO ratio decreases exponentially with increases in the C/O ratio (LG89). This could have interesting ramifications on the molecular abundances in chemically young galaxies. Observations with the Hubble Space Telescope have shown that the C/O abundance ratio increases with increasing metallicity in HII galaxies (Garnett et al. 1995). Therefore, we could expect to find lower C/O ratios and correspondingly larger O₂/CO ratios within dark molecular clouds in chemically young galaxies. Based on these simple ideas, the evolution of the O₂/CO abundance ratio as a function of metallicity in galaxies has been recently quantified for a variety of conditions and parameters governing the IMF and star formation histories (Frayser & Brown 1997 [FB97]). At low metallicities, FB97 calculate lower C/O ratios and enhanced O₂/CO ratios (O₂/CO ~ 1) within dark ($A_V > 5$) molecular clouds. At solar metallicities and above, the O₂/CO ratio is expected to decrease by several orders of magnitude.

Molecular oxygen has yet to be detected conclusively outside our solar system. Due to atmospheric attenuation, the ground-based Galactic searches have been limited to observing the rarer ¹⁶O¹⁸O isotope (Liszt & Vanden Bout 1985 [LV85]; Goldsmith et al. 1985; Combes et al. 1991 [C91]; Fuente et al. 1993; Maréchal et al. 1997 [M97]). The most sensitive Galactic studies have provided upper limits of approximately O₂/CO < 0.1. Extragalactic searches for the redshifted ¹⁶O₂ lines have provided more sensitive limits (O₂/CO < 0.01) but have also been

unsuccessful (Liszt 1985, Goldsmith & Young 1989 [GY89], C91, Liszt 1992 [L92]; Combes & Wiklind 1995). The most sensitive limit to date is $\text{O}_2/\text{CO} < 0.002$ (1σ) from an absorption line study toward the radio source B0218+357 (Combes, Wiklind, & Nakai 1997). All of these previous searches for O_2 have concentrated on chemically rich systems, or molecular clouds of unknown metallicity. Since the theoretical models suggest the possible enhancement of O_2 in chemically young galaxies, we have carried out a search for O_2 in metal-deficient galaxies.

From the literature, we have compiled a list of metal-poor ($Z \leq 0.5Z_\odot$) IRAS galaxies with redshifts of $z > 0.02$. There are only about 20 galaxies satisfying these constraints, which were primarily drawn from the samples of Salzer & MacAlpine (1988) and Dultzin-Hacyan, Masegosa, & Moles (1990). Unfortunately, most of these galaxies are relatively weak IRAS sources $I(100\mu\text{m}) \lesssim 1$ Jy, and none have reported CO detections. This is not terribly surprising since metal-deficient galaxies have lower amounts of dust. The metallicities for the galaxies in our sample were derived from their oxygen abundances calculated using standard HII region analysis techniques whenever the 4363Å [OIII] line was observed (Osterbrock 1989, case B). For galaxies with no 4363Å line, the techniques of McGaugh (1991) were used to estimate the oxygen abundance. In this initial study, we observed the strongest IRAS sources satisfying the metallicity and redshift constraints.

2. OBSERVATIONAL RESULTS

2.1. NRAO 12m Telescope

In April 1996 we observed five of the strongest IRAS galaxies which are known to be metal deficient and are at redshifts $z > 0.02$ with the NRAO¹ 12m telescope. The redshift constraint was required to permit the observations of the ground state transition of $^{16}\text{O}_2$ N,J= 1,1 \rightarrow 1,0 at a rest frequency of 118.7503 GHz. For all five of the galaxies, we first searched for $^{12}\text{CO}(1\rightarrow 0)$ line emission.

With the 12m telescope system, we used dual polarization SIS mixer receivers tuned to the frequency of the redshifted lines. The spectra were formed as total power differences between the source and a reference position 4' away in azimuth using a nutating subreflector to switch at a rate of 1.25 Hz. Each polarization was recorded using a 256×2 MHz filter bank spectrometer. The frequency setups were checked with observations of lines in Orion-KL and Sag-B2 (Turner 1989). Pointing was checked every 2–4 hours and was found to be accurate to within 10". Based on observations of Mars, we derived a conversion factor of 40 ± 8 Jy/K for the T_R^* temperature scale. This conversion factor assumes that the source is smaller than the 60" beam, which is valid for our sample of galaxies.

¹The National Radio Astronomy Observatory is a facility of the National Sciences Foundation operated under cooperative agreement by Associated Universities, Inc.

Table 1 shows the CO(1→0) results of the 12m observations. We detected CO(1→0) emission only in Mrk 109. The upper limits given in Table 1 for the CO(1→0) line strengths of the other four galaxies are 1σ rms, assuming a FWHM line width of 100 km s^{-1} . For the nondetections, the integration times range from 3 to 8 hours, and the system temperatures were from 250 K to 300 K. After the detection of CO(1→0) emission in Mrk 109, we searched for the 118.75 GHz $^{16}\text{O}_2(1,1 \rightarrow 1,0)$ line. From these observations we marginally detected a feature consistent with the O_2 line (Fig. 1). This feature was seen in both polarizations and in different subsets of the data. Interestingly, at the distance of Mrk 109 the $\text{O}_2(1,1 \rightarrow 1,0)$ line is redshifted to 115.22 GHz, which is very near the CO(1→0) rest frequency. However, the broad line-width ($\sim 200 \text{ km s}^{-1}$) rules out Galactic clouds as a possible origin of the 115.22 GHz feature, and there are no known low-redshift galaxies within or near the beam of the 12m observations. The velocity agreement for both features is encouraging (Fig. 1) and is consistent with both lines being associated with Mrk 109. Although 12 hours of source integration time were invested for each of these lines, the CO(1→0) and $\text{O}_2(1,1 \rightarrow 1,0)$ lines could only be considered tentatively detected with the 12m data. Follow-up observations with more sensitive telescopes were required to confirm the presence of these lines.

2.2. IRAM 30m Telescope

In July 1997 we obtained follow-up observations of Mrk 109 with the IRAM² 30m telescope. With the 30m telescope system, we simultaneously observed the redshifted CO(1→0) and $\text{O}_2(1,1 \rightarrow 1,0)$ lines. Each line was observed using a 512×1 MHz filter bank detector. The pointing of the telescope was checked every 2 hours with observations of 0923+392 and was found to have an accuracy of better than $5''$. The frequency setup of the observations was confirmed by test observations of IRC+10216. In three evenings we collected 6.3 hours of integration time on Mrk 109. Based on measurements of Mars taken each day, we derived a conversion factor of $8.8 \pm 1.6 \text{ Jy/K}$ for the observed T_A^* temperature scale.

Figure 2 shows the spectra for the redshifted CO(1→0) and $\text{O}_2(1,1 \rightarrow 1,0)$ lines. The CO(1→0) line was clearly detected, while the $\text{O}_2(1,1 \rightarrow 1,0)$ line was not. Since the optical size of Mrk 109 is less than the 30m beam size of $21''$, we conclude that the 115.22 GHz feature apparent in the 12m data does not arise from Mrk 109. We cannot rule out the possibility that this feature is associated with molecular gas outside the beam of the 30m, but within the 12m beam. One possibility, albeit improbable, is that the 12m feature is due to CO(1→0) emission from a previously undetected galaxy at $\sim 100 \text{ km s}^{-1}$. Most likely the 115.22 GHz feature seen in the 12m data is spurious.

²The Institut de RadioAstronomie Millimétrique (IRAM) is an international institute for research in millimeter astronomy, cofunded by the Centre National de la Recherche Scientifique, France, the Max Planck Gesellschaft, Germany, and the Instituto Geografico Nacional, Spain.

Based on the 30m data, we measure an integrated CO(1→0) line strength of $7.9 \pm 1.6 \text{ Jy km s}^{-1}$ over $cz = 9030 - 9230 \text{ km s}^{-1}$ for Mrk 109, which is 10 times larger than the integrated rms noise across the profile. The uncertainty in this measurement is dominated by the absolute flux calibration uncertainty of 18%. The 1σ upper limit to the O₂(1, 1 → 1, 0) line strength is $I(\text{O}_2)/I(\text{CO}) < 0.15$. We discuss the significance of this upper limit in §3.2.

2.3. OVRO Imaging

In January 1997, we obtained CO(1→0) and O₂(1, 1 → 1, 0) imaging observations of Mrk 109 with the six element Owens Valley Radio Observatory (OVRO) array.³ The CO(1→0) line was observed in the lower side-band, while the O₂(1, 1 → 1, 0) line was observed simultaneously in the upper side-band. Each line was observed using a 60×4 MHz digital correlator spectrometer centered on the redshifted frequencies of the lines. The phase center of the interferometric observations was the optical position of $\alpha(\text{B1950}) = 09^{\text{h}}19^{\text{m}}05^{\text{s}}.0$; $\delta(\text{B1950}) = +47^{\circ}27'28''$. These observations were carried out in a low resolution configuration (baselines ranging from 15–115 m), which provided a resolution of $4''$ using natural weighting. We obtained 20 hours of effective integration time on Mrk 109 spread over 4 separate nights. Observations of 3C 273 were used for passband and flux calibration. The observations of the nearby radio source 0923+392 were made every 20 minutes for gain calibration. The data were calibrated using the OVRO MMA software package, and the data analysis was accomplished using the NRAO AIPS software package.

Figure 3 shows a natural-weighted map of the CO(1→0) emission in Mrk 109 averaged over the velocity range showing CO emission in the 30m data. The CO(1→0) emission was unresolved and is spatially and kinematically consistent with the optical regions in Mrk 109 (Mazzarella & Boroson 1993). We measure an integrated CO(1→0) line strength of $6.9 \pm 1.8 \text{ Jy km s}^{-1}$ from the OVRO data which is consistent within uncertainties with the single-dish measurements. The line was detected at the 5.7σ level in the OVRO data, and a major contributor to the uncertainty of the CO line flux comes from the 20% flux calibration uncertainty. Figure 4 shows the CO(1→0) and O₂(1, 1 → 1, 0) spectra taken along the velocity axis of the data cubes at the peak position in the integrated CO map. The OVRO CO(1→0) line profile is very similar to that of the 30m. We find no evidence of a O₂ line in Mrk 109 from the OVRO data. No other features, besides CO(1→0) emission at the position of Mrk 109, were detected in the OVRO data cubes.

3. DISCUSSION

In this paper we report the detection of CO(1→0) emission in Mrk 109 as well as the nondetection of CO in four distant metal-deficient galaxies (Table 1). We estimate the amount of

³The OVRO Millimeter Array is operated as a radio astronomy facility by the California Institute of Technology.

molecular gas implied by these observations using the metallicity dependent relationship derived empirically by Wilson (1995). Wilson finds that the CO to H₂ conversion factor increases with decreasing metallicity as a -0.67 power law. We adopt this power law and calculate the molecular gas mass (including He) using

$$M(\text{H}_2) = 1.6 \times 10^4 \left(\frac{Z}{Z_\odot} \right)^{-0.67} \left(\frac{d}{\text{Mpc}} \right)^2 S_{\text{CO}} M_\odot, \quad (1)$$

where S_{CO} is the CO flux in Jy km s^{-1} (Wilson 1995). This relationship is consistent with simple theoretical arguments. In the low metallicity limit in which the CO emission becomes optically thin, we would expect the conversion factor to increase roughly linearly with decreasing metallicity (Sakamoto 1996). As the metallicity reaches the solar value, the CO emission becomes optically thick, and the conversion factor becomes independent of metallicity, ignoring other physical parameters. For global observations of metal-deficient galaxies, we could expect a mixture of CO optical depths and an effective power law for the conversion factor between 0 and -1 .

The $S(\text{CO})/S(100\mu\text{m})$ ratio for this sample of galaxies is significantly smaller than that for normal elliptical and spiral galaxies. By using the CO to IRAS flux correlation derived for normal galaxies (Bregman, Hogg, & Roberts 1992), we would expect CO(1 \rightarrow 0) fluxes of $20 - 30 \text{ Jy km s}^{-1}$, which are much larger than those found for these galaxies. This is not a new observational result for metal-deficient galaxies (e.g., Sage et al. 1992). Metallicity by itself, however, does not appear to explain this discrepancy. Assuming an intrinsic gas to dust ratio which increases linearly with decreasing metallicity (Issa, MacLaren, & Wolfendale 1990) and using the metallicity-corrected CO to H₂ conversion factor (as in eq.[1]), we would expect the $S(\text{CO})/S(100\mu\text{m})$ ratio to vary with $(Z/Z_\odot)^{-0.33}$. This dependence is much weaker than that which is observed. Clearly, more work is needed before we can gain a complete understanding of the low $S(\text{CO})/S(100\mu\text{m})$ ratios in metal-deficient galaxies. For the remaining of the paper, we focus on Mrk 109.

3.1. Molecular Gas in Mrk 109

The galaxy Mrk 109 is one of the more luminous metal-deficient starburst galaxies. It has an absolute magnitude of $M \sim -20$ which places it apart from the more typical low-luminosity metal-poor dwarf galaxies with $M \gtrsim -18$ (French 1980). Mrk 109 appears to be interacting with a nearby companion located approximately $10''$ west of Mrk 109. Both Mrk 109 and its companion are spectroscopically classified as HII galaxies and are separated by only 100 km s^{-1} in radial velocity (Mazzarella & Boroson 1993).

Figure 2 shows the velocities of the optical knots in Mrk 109 (labeled a, b, c, & d) and that of the companion galaxy (labeled A). The CO emission spans the full range of velocities given by the optical components, which is consistent with the interaction between Mrk 109 and the companion galaxy. Interestingly, the CO(1 \rightarrow 0) profile peaks at the velocity of the companion galaxy, while the CO emission is spatially consistent with the brightest central optical knot (b) in Mrk 109. The

interpretation of these results is not clear. It is possible that the kinematic center of Mrk 109 is offset from the brightest optical region and is more consistent with the average velocity of knots (a) and (d). Alternatively, the bulk of the gas observed may have been stripped from the companion galaxy (A). Unfortunately, we lack the sensitivity and resolution to provide a detailed kinematic study of the molecular gas in this system. However, we can deduce general characteristics such as the star-formation efficiency (SFE) and the gas fraction for this merger/starburst system.

Based on the 30m data, we derive a molecular gas mass of $M(\text{H}_2) = (3.8 \pm 0.7) \times 10^9 h_{75}^{-2} M_\odot$ for Mrk 109, using equation (1) where $h_{75} = H_o/(75 \text{ km s}^{-1} \text{ Mpc}^{-1})$. This is a relatively large amount of molecular gas for a metal-deficient galaxy and is similar to the total amount of molecular gas estimated for the Milky Way ($2 \times 10^9 M_\odot$, Solomon & Rivolo 1987). The dynamical mass contained within the CO emission regions is $M_{dyn} = R(\Delta V/[2 \sin(i)])^2/G$, where ΔV is the observed FWZI line width of 200 km s^{-1} . The resolution of the OVRO data places an upper limit on the size of the CO emission region of $R < 1.2 h_{75}^{-1} \text{ kpc}$. The inclination of Mrk 109 is unknown. Assuming an intrinsic axial ratio of one, the observed optical axial ratio (Mazzarella & Boroson 1993) implies an inclination of $i \sim 61^\circ$. Using the above numbers, we calculate a dynamical mass of $M_{dyn} < 3.6 \times 10^9 h_{75}^{-1} M_\odot$. These results suggest a gas fraction of approximately unity within the central regions of Mrk 109. Granted, given the uncertainties in the CO to H_2 conversion factor and inclination, the gas fraction may be lower. If we, nevertheless, take these results at face value, the large calculated gas fraction is consistent with a young starburst, where the majority of the gas has yet to be consumed by the ongoing star formation.

By using the $\text{H}\alpha$ line luminosity of Mrk 109 (Mazzarella, Bothun, & Boroson 1991), we estimate a total star-formation rate (SFR) of $2 M_\odot \text{ yr}^{-1}$ (Kennicutt 1983). This value is consistent with the SFR expected from its far infrared luminosity, assuming the relationship given by Sage et al. (1992). In addition, the derived SFR is also consistent with the upper limit implied from the radio data. Mrk 109 has not been detected at cm wavelengths. The data from the NRAO VLA Sky Survey (Condon et al. 1998) implies a flux density of less than 1 mJy (2σ) at 1.4 GHz. Using this value we derive an upper limit to the total SFR of approximately $2 M_\odot \text{ yr}^{-1}$, assuming non-thermal radio emission from supernovae remnants and renormalizing the formulae of Condon (1992) to match the IMF of Kennicutt (1983). The consistency of the radio, infrared, and optical data indicates that the SFR has not been seriously underestimated due to high-extinction regions that are hidden at optical wavelengths.

The star-formation efficiency can be defined as the the ratio of the SFR to the amount of molecular gas. For Mrk 109, we find an implied efficiency of only $\text{SFE} \sim 0.5 \text{ Gyr}^{-1}$, which is an order of magnitude lower than that typically found for starburst galaxies (Sage et al. 1992). Assuming a constant SFR, this would translate into a gas depletion time scale of 2 Gyr for Mrk 109. The SFR, SFE, and gas depletion time scale of Mrk 109 are, hence, more similar to those found for normal spiral galaxies than starburst systems. At first glance, these results could appear contradictory with a merger scenario where we expect to typically find high SFRs (e.g., Mihos, Richstone, & Bothun 1992). However, most previously studied merger systems are

older metal-rich, IRAS luminous starbursts (e.g., Sanders, Scoville, & Soifer 1991). Mrk 109 is a low metallicity system whose ISM has undergone significantly less processing. It is possible that Mrk 109 is a young interacting system still in the process of gaseous infall into the central starburst region which could explain its current low SFE.

3.2. Constraining the O₂/CO Ratio for Sub-solar Metallicities

The major goal of this study is to constrain the O₂/CO abundance ratio for chemically young systems. Previous searches for O₂ emission have been directed toward CO bright sources, such as nearby giant molecular cloud (GMC) cores or the centers of bright IRAS galaxies (§1). In this paper, we present the first O₂/CO abundance limit for a metal-deficient galaxy.

The observed intensity limit for the O₂(1, 1 → 1, 0) line in Mrk 109 is $I_{\text{O}_2}/I_{\text{CO}} < 0.15$ (§2.2). By combining equation (1) with the expression given by Liszt (1992), we can relate the observed intensity ratio to a column density abundance ratio with the following expression (FB97):

$$\frac{I(\text{O}_2)}{I(\text{CO})} = 0.68 \left(\frac{N(\text{O}_2)}{N(\text{CO})} \right) \left(\frac{Z}{Z_\odot} \right)^{0.33} \left(\frac{30 \text{ K}}{T} \right). \quad (2)$$

The $N(\text{O}_2)/N(\text{CO})$ ratio is the column density abundance ratio averaged over the telescope beam. It is related to the intrinsic O₂/CO abundance ratio by $N(\text{O}_2)/N(\text{CO}) = (\text{O}_2/\text{CO})(f_{\text{O}_2}/f_{\text{CO}})$, where $f_{\text{O}_2}/f_{\text{CO}}$ is the ratio of the filling factors of the O₂ and CO emission regions within the telescope beam. If the CO and O₂ emission regions are coextensive, then $f_{\text{O}_2}/f_{\text{CO}} = 1$. Although this has been assumed for all previous O₂ studies, it may not be valid. For now we adopt $f_{\text{O}_2}/f_{\text{CO}} = 1$ and discuss the applicability of this assumption later.

By adopting $T = 30 \text{ K}$ and using equation (2), we calculate $N(\text{O}_2)/N(\text{CO}) < 0.31$ (1σ) for Mrk 109. To determine the significance of this upper limit, we have compiled a list of observational limits in regions of known metallicities and/or O/C abundance ratios. Figure 5 compares the observational upper limits of the O₂/CO ratio with theoretical expectations as a function of the O/C ratio. We first summarize the data displayed in Figure 5, and then we discuss several implications of the data.

The analytical fits in Figure 5 were made to the steady-state and early-time solutions of LG89 and MH90 (FB97). The steady-state solutions represent the equilibrium values achieved in the chemistry models after $t > 10^7 \text{ yr}$, while the early-time solutions are for $t \sim 10^5 \text{ yr}$. The LG89 solutions are for Galactic clouds, and the MH90 solutions are for clouds in the LMC and SMC. Both sets of calculations assume dark clouds ($A_V \sim 10$). Figure 5 shows the effects of different processes on the steady-state solutions, such as grain surface adsorption and desorption (BLG95), turbulent diffusion (Xie, Allen, & Langer 1995 [XAL95]), and mixing (Pineau des Forêts, Flower, & Chièze 1992 [PFC92]).

Most of the previous searches for O₂ have been made for regions of unknown O/C abundance

ratios and uncertain metallicities, and the previous comparisons between the observational limits of the O_2/CO ratio and the theoretical calculations generally assume a solar O/C abundance ratio. Since the O_2/CO ratio is strongly nonlinear with the O/C ratio near solar metallicities, accurate estimates of the O/C ratio are required in order to constrain the theoretical models. We find only three sources in the literature with both O_2/CO upper limits and a direct estimate of the O/C ratio (Orion, L134N, and NGC 7674). All three of these sources have sufficiently low O/C ratios that their observational O_2/CO limits do not contradict the theoretical estimates (Fig. 5). In Figure 5 we adopt the average nebular abundance ratio of $\text{O}/\text{C}= 1.4$ for Orion (Cunha & Lambert 1994 [CL94]). For the molecular complex L134N, we display the data at the position of the peak in the SO map ($-1'.4, -0'.8$) which has the highest inferred O/C ratio in L134N ($\text{O}/\text{C}= 0.83$, Swade 1989 [S89]). The O/C ratio for the Seyfert galaxy NGC 7674 was based on the best model fit to its IUE spectra (Kraemer et al. 1994 [K94]). For the data point marked with the symbol “*” in Figure 5, we assume that the Galactic molecular regions searched for O_2 (LV85; M97) have O/C ratios in agreement with typical values observed in the diffuse ISM of $\text{O}/\text{C}\simeq 1.25 - 2.5$ (Cardelli et al. 1993 [C93]). The assumption of similar O/C ratios in the diffuse ISM and in regions of high extinction (e.g., cores of GMCs) may not be valid, especially considering the results for L134N where $\text{O}/\text{C} < 1$. For the galaxies NGC 6090 and Mrk 109, we estimate the O/C ratio assuming the relationship seen between the metallicity and the C/O ratio (FB97; Garnett et al. 1995). The metallicity for NGC 6090 was derived by Storchi–Bergmann, Calzetti, & Kinney (1994) [S94] using indirect methods consistent with those of McGaugh (1991) and is fairly uncertain (0.15 dex error). The metallicity for Mrk 109 is more reliable (Table 1) since the 4363\AA [OIII] line was observed (French 1980). The uncertainties in the O/C ratio derived for Mrk 109 and NGC 6090 reflect the scatter in the data for the relationship between metallicity and the C/O ratio (see Fig. 7 of FB97).

All $^{16}\text{O}_2/\text{CO}$ abundance limits shown in Figure 5 are 2σ . For Galactic sources, the data are based on observations of the $^{16}\text{O}^{18}\text{O}$ molecule and standard isotopic ratios are assumed. Estimated gas temperatures are used for the individual Galactic sources (e.g., $T = 10 - 40$ K, M97) to account for the temperature dependency on the O_2 abundance. For the extragalactic sources, we assumed $T = 30$ K. We used equation (2) to derive the O_2/CO abundance ratio for the galaxies Mrk 109 and NGC 6090. For NGC 7674 we used the Galactic CO to H_2 conversion factor; i.e., we removed the $(Z/Z_\odot)^{0.33}$ term from equation (2) which is applicable for only metal-deficient galaxies. It was assumed that the filling factors of the O_2 and CO emission regions are similar ($f_{\text{O}_2}/f_{\text{CO}} \sim 1$) for all of the limits in Figure 5.

By including the data for Mrk 109, we can begin to discuss several implications for the O_2/CO abundance ratio over a relatively wide range of O/C ratios (Fig. 5). If we assume that Galactic molecular clouds have a solar abundance ratio of $\text{O}/\text{C}\simeq 2$ (Grevesse, Noels, & Sauval 1996), the observations contradict the standard steady-state solutions for molecular chemistry. Several authors have already summarized various possible mechanisms which could account for the discrepancy (see FB97; M97). One promising mechanism is mixing. When the dense interior gas mixes with the outer layers, the clouds do not reach their steady-state chemistry solutions,

but have solutions similar to those derived at early times. For these models the O_2/CO ratios are expected to be lowered by several orders of magnitude at solar abundances due to a higher fraction of the carbon in atomic and ionized species (FB97). For metal-deficient systems these effects could be less important since the O/C ratios are larger. In fact, for $O/C \gtrsim 10$ the early-time solutions begin to converge with those of steady-state. In this scenario the metal-deficient galaxies could be the best sources to search for O_2 .

The observations of Mrk 109 provide us with the first probe of a metal-deficient system. The O_2/CO upper limit for Mrk 109 is lower than the expected steady-state solutions (Fig. 5). As stated earlier, the theoretical solutions were derived assuming dark molecular clouds. Since the photodissociation rate for O_2 is larger than that for CO (van Dishoeck 1988), the global averaged O_2/CO abundance ratios could be significantly lower than the dark cloud solutions (FB97). Therefore, at low metallicities we have two competing tendencies affecting the global O_2/CO ratio. On one hand, the production of O_2 is enhanced due to the higher O/C ratios, but on the other hand the O_2 molecules are more susceptible to photodissociation. The effect that photodissociation has on the global O_2/CO abundance ratio depends on the fraction of the molecular gas residing in dark clouds. Significant O_2 emission is only expected from regions with $A_V \gtrsim 5$, while CO emission can arise from regions with lower values of extinction (FB97). Since the CO emission is thought to be more pervasive than the O_2 emission, we would expect relative filling factors of $f_{O_2}/f_{CO} < 1$ for extragalactic observations of a collection of clouds. Hence, the standard assumption of $f_{O_2}/f_{CO} = 1$ is not valid in general. Assuming spherical molecular clouds, we estimate that $M(H_2)_{dark}/M(H_2)_{total} \simeq (f_{O_2}/f_{CO})^{1.5}$ based on the work of FB97. If we use the steady-state theoretical solutions, we would expect $O_2/CO = 1.3$ for the dark cloud regions ($A_V > 5$) in Mrk 109. The 1σ upper limit on the $N(O_2)/N(CO)$ ratio for Mrk 109 would then suggest $f_{O_2}/f_{CO} < 0.24$ and $M(H_2)_{dark}/M(H_2)_{total} < 0.12$. In summary, either most of the molecular gas does not reside in dark clouds in Mrk 109, or the steady-state solutions do not apply for Mrk 109.

By using the models of FB97 which assume the size-density relationship and the GMC mass function found for Galactic clouds, we estimate $f_{O_2}/f_{CO} \simeq 0.05$ for regions with a metallicity similar to that of Mrk 109. This value is calculated from the ratio of the volume-weighted mass fractions of molecular hydrogen traced by the O_2 and CO molecules; $f_{O_2}/f_{CO} = (M[H_2]^{O_2}/M[H_2]^{CO})^{2/3}$ (FB97). Arguably, molecular clouds at low metallicities may be comprised of higher density clumps than those found for Galactic GMCs, given the studies of the LMC and SMC (Lequeux et al. 1994). In such a case, the above value for the f_{O_2}/f_{CO} ratio should be thought of as a lower limit. The likely value of f_{O_2}/f_{CO} for Mrk 109 is, therefore, $0.05 < f_{O_2}/f_{CO} < 0.24$. In this context, the observational O_2/CO limit for Mrk 109 is not that restrictive on the models of molecular gas-phase chemistry in dark clouds. Both the steady-state and early-time solutions are possible for values of $f_{O_2}/f_{CO} \sim 0.1$.

4. CONCLUSIONS

In this paper, we report the nondetection of CO(1→0) emission in four distant metal-deficient galaxies and the detection of CO emission in Mrk 109. The CO(1→0) observations of Mrk 109 imply the presence of $4 \times 10^9 M_{\odot}$ of molecular gas within the central few kpc of Mrk 109. The observational data favor a recent interaction of Mrk 109 with a nearby companion which has induced a starburst in the central regions of Mrk 109. The low metallicity, high gas fraction, and the kinematics are consistent with a young starburst.

Based on the competing photodissociation and chemistry effects, we expect the largest global O₂/CO ratios for systems with metallicities in the range of $0.1 < Z/Z_{\odot} < 0.5$ (FB97). Although the metallicity of Mrk 109 falls within this optimal range, we fail to detect O₂ emission in Mrk 109. The observed intensity upper limit is $I(\text{O}_2)/I(\text{CO}) < 0.15$. These observations provide the first constraint on the abundance of O₂ in a metal-deficient galaxy. We derive a column density abundance limit of $N(\text{O}_2)/N(\text{CO}) < 0.31$ for Mrk 109. These results suggest that most of the molecular gas in Mrk 109 does not reside in dark clouds, and/or that the gas-phase steady-state chemistry models do not apply for Mrk 109. It would be challenging to significantly improve the O₂/CO limit for chemically young environments derived from this work with current ground-based instrumentation. Future observations with satellites, such as ODIN (Hjalmarson 1997), of the LMC and SMC should provide more useful limits.

We are grateful to the staff of the NRAO 12m telescope, IRAM 30m telescope, and OVRO mm-array who made these observations possible. We thank the referee C. Wilson for constructive suggestions concerning the manuscript. This research has made use of the NASA/IPAC Extragalactic Database (NED) which is operated by the Jet Propulsion Laboratory, California Institute of Technology, under contract with the National Aeronautics and Space Administration. This research was supported in part by a grant to E.R.S. from the Natural Sciences and Engineering Research Council of Canada and by the National Science Foundation grant AST-96-13717 to the Owens Valley Radio Observatory.

REFERENCES

- Arnault, P., Kunth, D., Casoli, F., & Combes, F. 1988, *A&A*, 205, 41
Arimoto, N., Sofue, Y., & Tsujimoto, T. 1996, *PASJ*, 48, 275
Bergin, E. A., Langer, W. D., & Goldsmith, P. F. 1995 (BLG95), *ApJ*, 441, 222
Bregman, J. N., Hogg, D. E., & Roberts, M. S. 1992, *ApJ*, 387, 484
Campos-Aguilar, A., Moles, M., & Masegosa, J. 1993, *AJ*, 106, 1784
Cardelli, J. A., Mathis, J. S., Ebbets, D. C., & Savage, B. D. 1993 (C93), *ApJ*, 402, L17

- Combes, F. 1985, in *Star-Forming Dwarf Galaxies*, ed. D. Kunth, T. X. Thuan, & J. Tran Thanh Van (Gif Sur Yvette: Frontieres), 307
- Combes, F., Casoli, F., Encrenaz, P., Gerin, M., & Laurent, C. 1991 (C91), *A&A*, 248, 607
- Combes, F., & Wiklind, T. 1995, *A&A*, 303, L61
- Combes, F., Wiklind, T., & Nakai, N. 1997, *A&A*, 327, L17
- Condon, J. J. 1992, *ARA&A*, 30, 575
- Condon, J. J., et al. 1998, *AJ*, submitted
- Cunha, K., & Lambert, D. L. 1994 (CL94), *ApJ*, 426, 170
- Dultzin-Hacyan, D., Masegosa, J., & Moles, M. 1990, *A&A*, 238, 28
- Frayer, D. T., & Brown, R. L. 1997 (FB97), *ApJS*, 113, 221
- French, H. B. 1980, *ApJ*, 240, 41
- Fuente, A., Cernicharo, J., García-Burillo, S., & Tejero, J. 1993, *A&A*, 275, 558
- Garnett, D. R., Skillman, E. D., Dufour, R. J., Peimbert, M., Torres-Peimbert, S., Terlevich, R. J., Terlevich, E., & Shields, G. A. 1995, *ApJ*, 443, 64
- Goldsmith, P. F., Snell, R. L., Erickson, N. R., Dickman, R. L., Schloerb, F. P., & Irvine, W. M. 1985, *ApJ*, 289, 613
- Goldsmith, P. F., & Young, J. S. 1989 (GY89), *ApJ*, 341, 718
- Graedel, T. E., Langer, W. D., & Frerking, M. A. 1982, *ApJS*, 48, 321
- Grevesse, N., Noels, A., & Sauval, A. J. 1996, in *Cosmic Abundances*, ed. S. S. Holt & G. Sonneborn (San Francisco: Astronomical Society of the Pacific), 117
- Herbst, E., & Leung, C. M. 1989 (HL89), *ApJS*, 69, 271
- Hjalmarson, Å. 1997, in *CO: Twenty-five Years of Millimeter-wave Spectroscopy*, ed. W. B. Latter et al. (Dordrecht: Kluwer), 227
- Israel, F. P. 1997, *A&A*, 328, 471
- Israel, F. P., Tacconi, L. J., & Baas F. 1995, *A&A*, 295, 599
- Issa, M. R., MacLaren, I., & Wolfendale, A. W. 1990, *A&A*, 236, 237
- Kennicutt, R. C., Jr. 1983, *ApJ*, 272, 54
- Kraemer, S. B., Wu, C.-C., Crenshaw, D. M., & Harrington, J. P. 1994 (K94), *ApJ*, 435, 171
- Kunth, D. & Sevre, F. 1985, in *Star-Forming Dwarf Galaxies*, ed. D. Kunth, T. X. Thuan, & J. Tran Thanh Van (Gif Sur Yvette: Frontieres), 331
- Langer, W. D., & Graedel, T. E. 1989 (LG89), *ApJS*, 69, 241
- Lequeux, J., Le Bourlot, J., Pineau des Forêts, G., Roueff, E., Boulanger, F., & Rubio, M. 1994, *A&A* 292, 371

- Liszt, H. S. 1985, ApJ, 298, 281
- Liszt, H. S. 1992 (L92), ApJ, 386, 139
- Liszt, H. S., & Vanden Bout, P. A. 1985 (LV85), ApJ, 291, 178
- Maréchal, P., Pagani, L., Langer, W. D., & Castets, A. 1997 (M97), A&A, 318, 252
- Mazzarella, J. M., & Boroson, T. A. 1993, ApJS, 85, 27
- Mazzarella, J. M., Bothun, G. D., & Boroson, T. A. 1991, AJ, 101, 2034
- McGaugh, S. S. 1991, ApJ, 380, 140
- Mihos, J. C., Richstone, D. O., & Bothun, G. D. 1992, ApJ, 400, 153
- Millar, T. J., & Herbst, E. 1990 (MH90), MNRAS, 242, 92
- Osterbrock, D. E. 1989, *Astrophysics of Gaseous Nebulae and Active Galactic Nuclei* (Mill Valley: Univ. Science Books)
- Pineau des Forêts, G., Flower, D. R., & Chièze, J.-P., 1992 (PFC92), MNRAS, 256, 247
- Rubio, M. 1997, in *CO: Twenty-five Years of Millimeter-wave Spectroscopy*, ed. W. B. Latter et al. (Dordrecht: Kluwer), 265
- Sage, L. J., Salzer, J. J., Loose, H.-H., & Henkel, C. 1992, A&A, 265, 19
- Sakamoto, S. 1996, ApJ, 462, 215
- Salzer, J. J. & MacAlpine, G. M. 1988, AJ, 96, 1192
- Sanders, D. B., Scoville, N. Z., & Soifer, B. T. 1991, ApJ, 370, 158
- Solomon, P. M., & Rivolo, A. R. 1987, in *The Galaxy*, ed. G. Gilmore & B. Carswell (Dordrecht: Reidel), 105
- Storchi-Bergmann, T., Calzetti, D., & Kinney, A. L. 1994 (S94), ApJ, 429, 572
- Swade, D. A. 1989 (S89), ApJ, 345, 828
- Terlevich, R., Melnick, J., Masegosa, J., Moles, M., & Copetti, M. V. F. 1991, A&AS, 91, 285
- Turner, B. E. 1989, ApJS, 70, 539
- van Dishoeck, E. F. 1988, in *Rate Coefficients in Astrochemistry*, ed. T. J. Millar & D. A. Williams (Dordrecht: Kluwer), 49
- Wilson, C. D. 1995, ApJ, 448, L97
- Xie, T., Allen, M., & Langer, W. D. 1995 (XAL95), ApJ, 440, 674

Fig. 1.— The CO(1→0) and O₂(1,1 → 1,0) spectra of Mrk 109 observed with the NRAO 12m telescope. The heliocentric velocities of the optical knots in Mrk 109 are labeled with “a,b,c, & d”, while the nearby companion galaxy has a velocity labeled with “A” (Mazzarella & Boroson 1993). The data have been smoothed to 50 km s⁻¹, and the 1σ rms is 19 mJy and 25 mJy for the CO and O₂ data, respectively. The apparent O₂(1,1 → 1,0) feature is most likely spurious, given the results shown in Fig. 2&4.

Fig. 2.— The CO(1→0) and O₂(1,1 → 1,0) spectra of Mrk 109 observed with the IRAM 30m telescope. The labels for the velocities of optical regions are the same as in Figure 1. The data have been smoothed to 25 km s⁻¹, and the 1σ rms is 11 mJy and 16 mJy for the CO and O₂ data, respectively. No O₂(1,1 → 1,0) emission is detected.

Fig. 3.— The integrated CO(1→0) map of Mrk 109 observed with the OVRO mm–array. The CO emission was integrated over the velocity range showing CO emission in the 30m spectrum (Fig. 2). The positional offsets are relative to the optical position of Mrk 109, and the location of the CO emission is consistent with the brightest optical regions in Mrk 109 (Mazzarella & Boroson 1993). The 1σ rms is 1.2 Jy km s⁻¹/beam, and the contour levels are -2.5σ, 2.5σ, 3.5σ, 4.5σ, & 5.5σ. The synthesized beam size is shown at the lower left.

Fig. 4.— The CO(1→0) and O₂(1,1 → 1,0) spectra of Mrk 109 at the peak position in the integrated CO map (Fig. 3). The labels for the velocities of optical regions are the same as in Figure 1. The data have been smoothed to 12 MHz (~ 30 km s⁻¹), and the 1σ rms is 14 mJy/beam and 19 mJy/beam for the CO and O₂ data, respectively. No O₂(1,1 → 1,0) emission is detected.

Fig. 5.— The O₂/CO ratio as a function of the O/C ratio. Observational upper limits of the O₂/CO ratio (2σ) are shown along with theoretical data from several different time dependent molecular chemistry models (see text). Analytical fits are shown for the steady–state solutions of LG89 and MH90 and for the early–time solutions of MH90. The data point for Mrk 109 is the first observational constraint for the O₂/CO ratio in low–metallicity molecular gas.

Table 1. CO(1→0) Observations at the 12m Telescope

Name	Redshift (z)	Metallicity ^a (O/H)/(O/H) _⊙	S(100μm) (Jy)	CO(1→0) (Jy km s ⁻¹)	M(H ₂) ^b (10 ⁹ h ₇₅ ⁻² M _⊙)
UM 17	0.0274	0.31 ^c	1.6 ^d	< 2.4 ^e	< 1.0
Haro 15	0.0216	0.50 ^f	2.0 ^g	< 1.5 ^e	< 0.3
Mrk 109	0.0306	0.36 ^h	1.1 ^g	9.2 ± 3.2 ⁱ	4.3 ± 1.5
Mrk 162	0.0215	0.11 ^h	1.6 ^g	< 2.1 ^e	< 1.1
UM 603	0.0300	0.42 ^j	1.5 ^k	< 2.2 ^e	< 0.9

Note. — ^aBased on a solar oxygen abundance of $12 + \log(\text{O}/\text{H}) = 8.87$ (Grevesse et al. 1996). ^bMolecular gas mass calculated assuming the metallicity dependent CO to H₂ conversion factor of Wilson (1995); $h_{75} = H_o/(75 \text{ km s}^{-1} \text{ Mpc}^{-1})$. ^cMetallicity estimated from the data of Terlevich et al. (1991) using the method of McGaugh (1991). ^dDultzin–Hacyan et al. (1990). ^e1σ rms assuming 100 km s⁻¹ line width. ^fStorchi–Bergmann et al. (1994). ^gNASA/IPAC Extragalactic Data Base. ^hKunth & Sevre (1985). ⁱMeasured over 8880–9220 km s⁻¹ with the uncertainty calculated from a combination of the 28% rms uncertainty and the 20% absolute flux calibration uncertainty. ^jCampos–Aguilar, Moles, & Masegosa (1993). ^kSalzer & MacAlpine (1990).

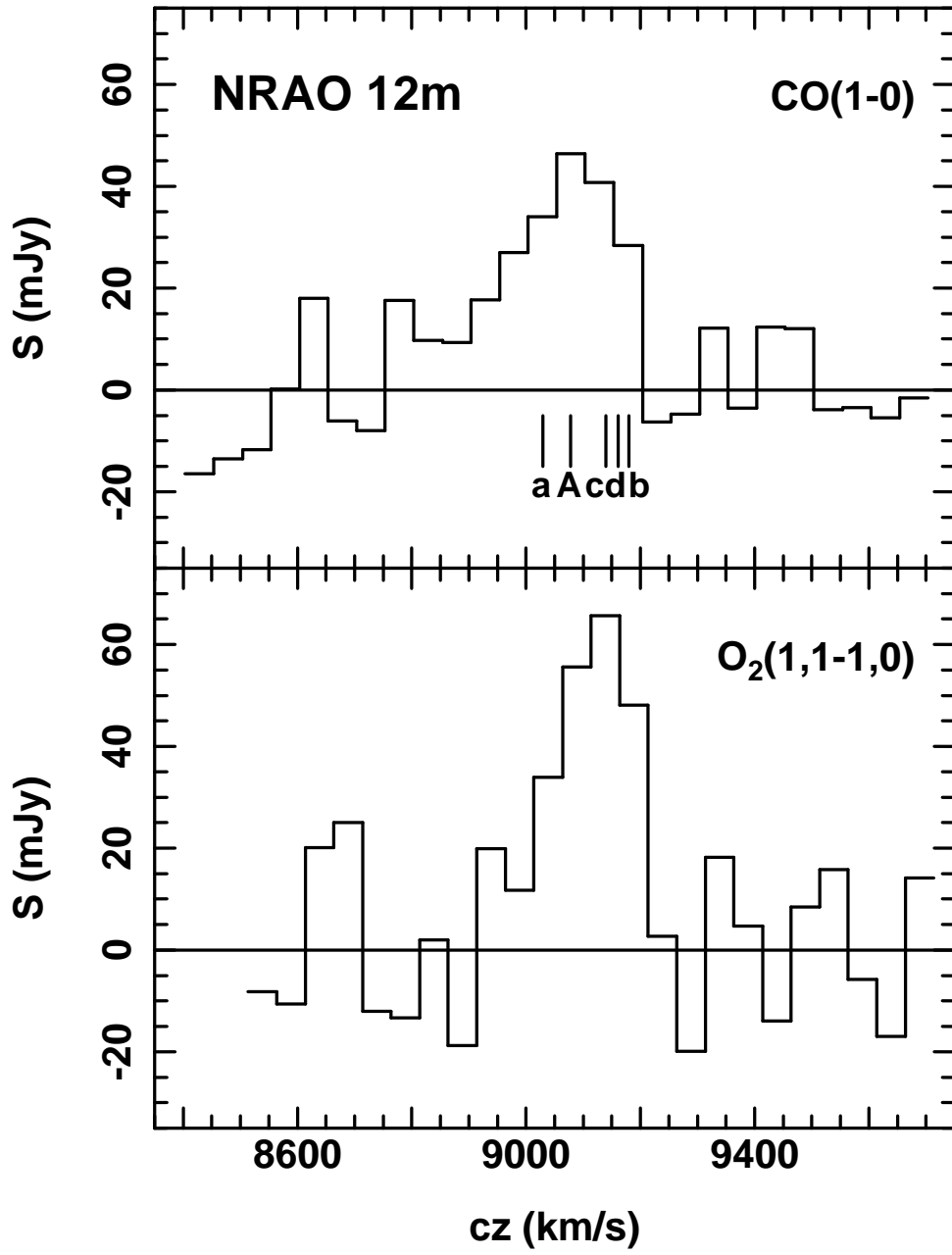


Fig. 1.—

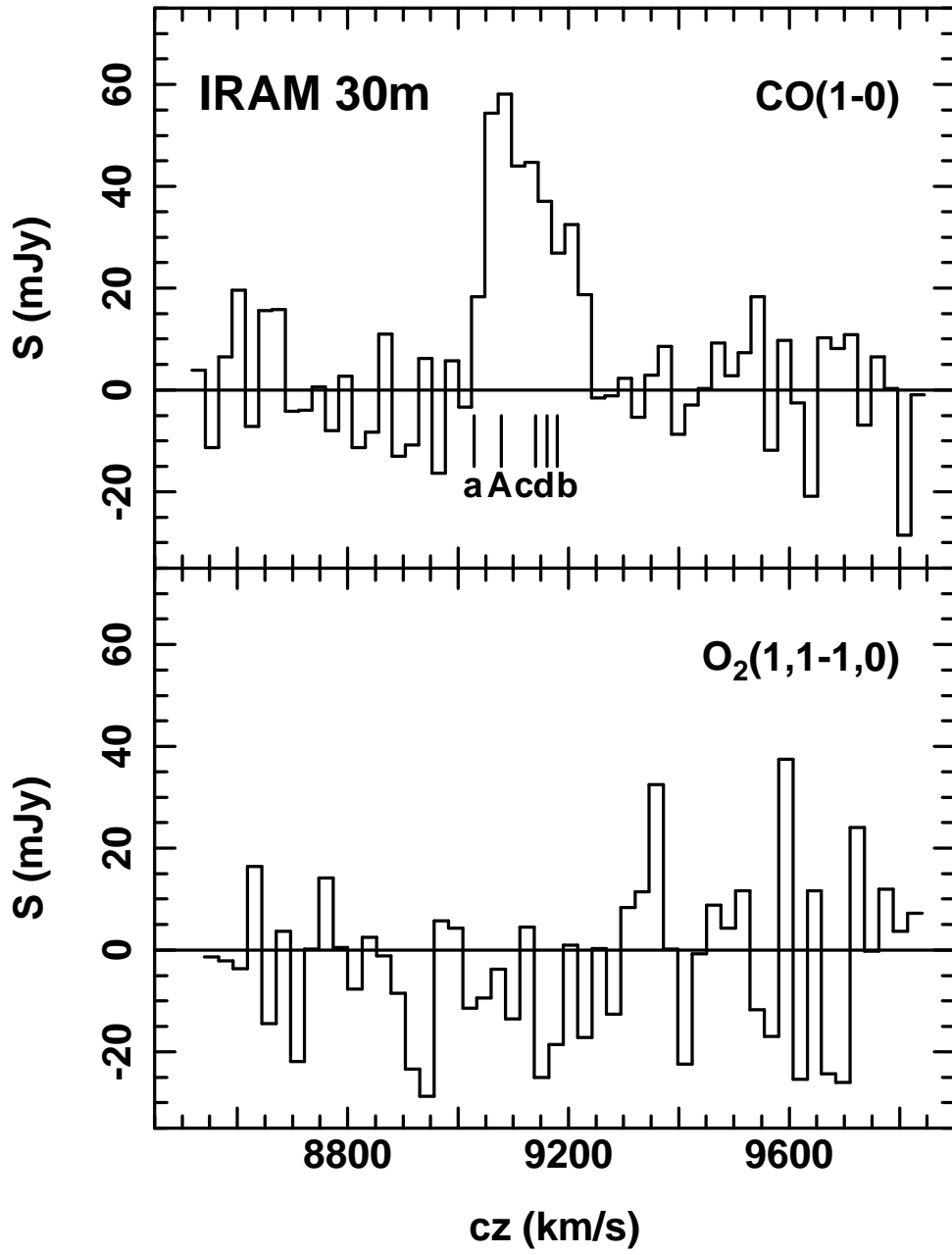


Fig. 2.—

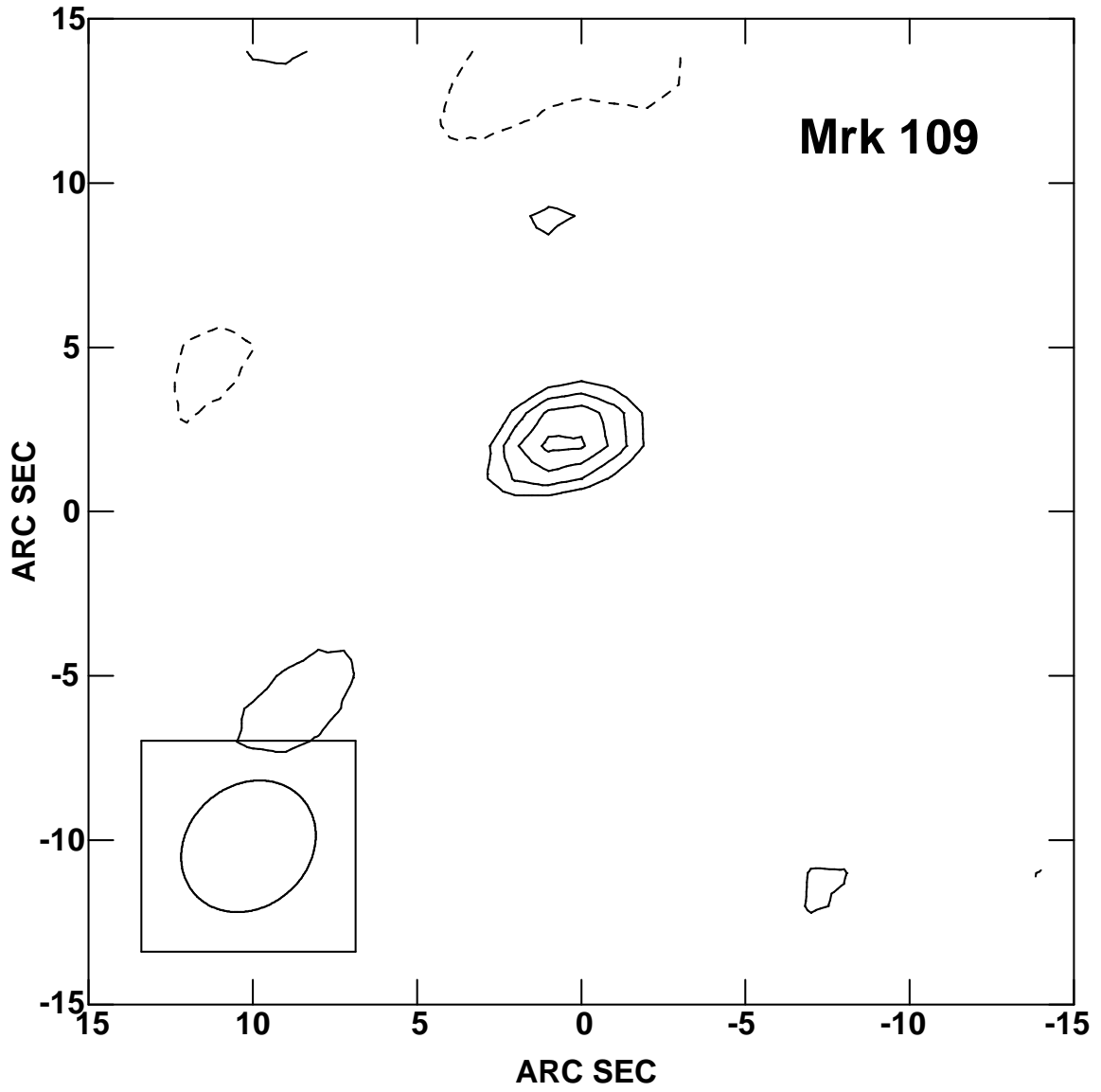


Fig. 3.—

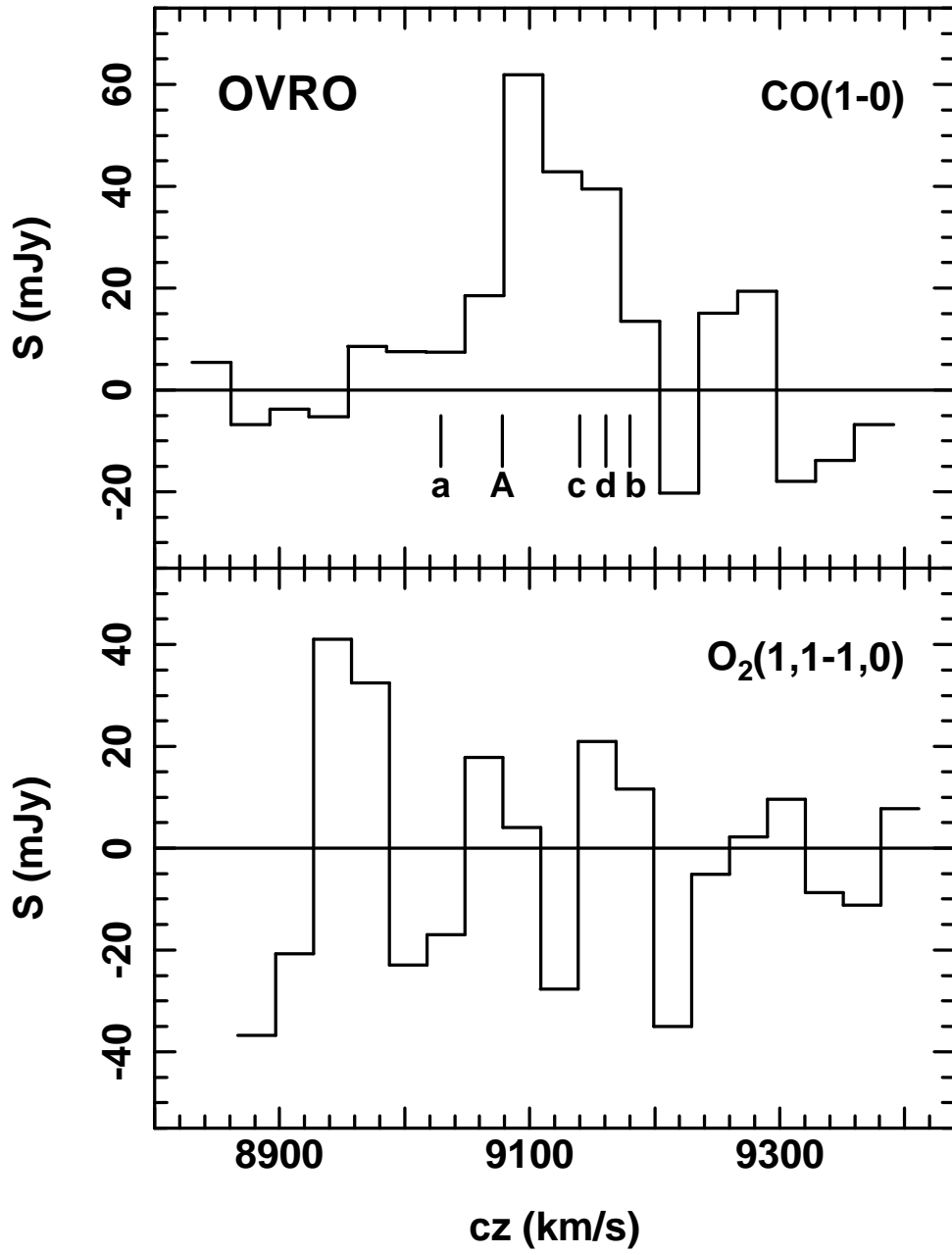


Fig. 4.—

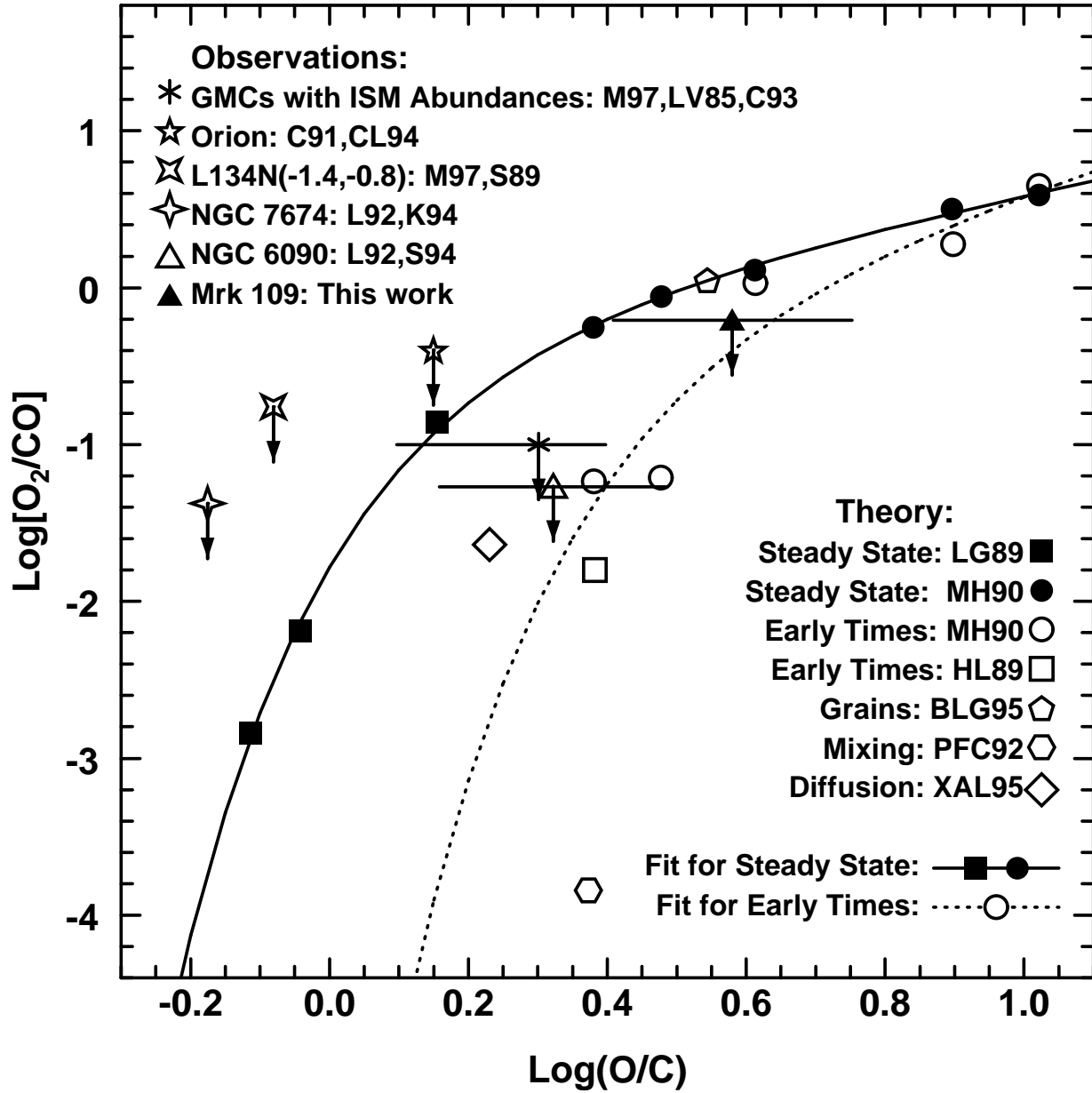


Fig. 5.—